IEEE Access
Multidisciplinary ⋮ Rapid Review ⋮ Open Access Journal

Received 14 March 2023, accepted 10 April 2023, date of publication 11 May 2023, date of current version 6 July 2023.

Digital Object Identifier 10.1109/ACCESS.2023.3275529

RESEARCH ARTICLE

Non-Intrusive Head Movement Control for Powered Wheelchairs: A Vision-Based Approach

SOTIRIOS CHATZIDIMITRIADIS[1], SABER MIRZAEE BAFTI[1], AND KONSTANTINOS SIRLANTZIS[2], (Member, IEEE)

[1]Intelligent Interactions Research Group, School of Engineering, University of Kent, CT2 7NT Canterbury, U.K.
[2]School of Engineering, Technology and Design, Canterbury Christ Church University (CCCU), CT1 1QU Canterbury, U.K.

Corresponding author: Sotirios Chatzidimitriadis (sc866@kent.ac.uk)

This work was supported by the Assistive Devices for empowering disAbled People through robotic Technologies (ADAPT) project. ADAPT was selected for funding by the INTERREG VA France (Channel) England Programme which is co-financed by the European Regional Development Fund (ERDF). The European Regional Development Fund (ERDF) is one of the main financial instruments of the European Unions (EU) cohesion policy.

This work involved human subjects in its research. Approval of all ethical and experimental procedures and protocols was granted by the University of Kent's Central Research Ethics Advisory Group under Application Ref. CREAG074-07-2021.

ABSTRACT Joystick is the most common wheelchair controlling interface, however, it might not be applicable for cases of severely disabled people, for example quadriplegic users. The few solutions currently available on the market, such as the four switches on the headrest, the sip-n-puff, or the tongue drive system, can be cumbersome to use, while they offer limited control to the user. For such cases, a vision-based head-controlled wheelchair is a unique alternative solution, which despite its benefits, has not been equally well studied. In this work, we propose and evaluate a novel method for operating an Electric Powered Wheelchair (EPW) via head movements in a non-invasive way. This is based on computer vision techniques and Deep Learning to estimate accurately the orientation of the user's head. It allows calibration for individual users and driving in a continuous navigation space as opposed to the discrete commands imposed by alternatives such as head switches. Our approach enables the design of an efficient and cost-effective solution utilising a simple RGB camera that captures the user's face orientation. Our system is implemented and tested real-time on an EPW using its existing commercial controller, while it can work with any commercial controller the manufacturer allows interfacing with (i.e., a direct plugin). Performance is evaluated through trials conducted with healthy participants. The results (96% successful track completion) show that our head driving system can be reliably used as an alternative solution to the conventional joystick interface, with only a small trade-off in travelling time and distance (reduction by 9.4% and 21% respectively). The participants' experience in terms of mental and physical load, subjectively assessed following the trials, suggests relatively low mental and physical demand imposed by our system. Users also expressed high confidence in the system's performance indicating trust to the safety aspects of our implementation. Analysis of our findings and experimental observations provide a new knowledge base for potential system improvements and future designs.

INDEX TERMS Head-controlled wheelchair, spinal cord injury, assistive technologies, head tracking, robotic wheelchair, gesture-based control.

I. INTRODUCTION

Loss of personal mobility due to spinal cord injury is a major challenge in the lives of affected individuals. According to a wide study conducted in the U.S. [1], about 45% of Spinal Cord-Injured (SCI) people end up with incomplete quadriplegia, and 13.3% end up with complete quadriplegia, rendering all four limbs paralyzed. While motorized wheelchairs have been instrumental in promoting independence among disabled individuals, traditional

The associate editor coordinating the review of this manuscript and approving it for publication was Tao Liu.

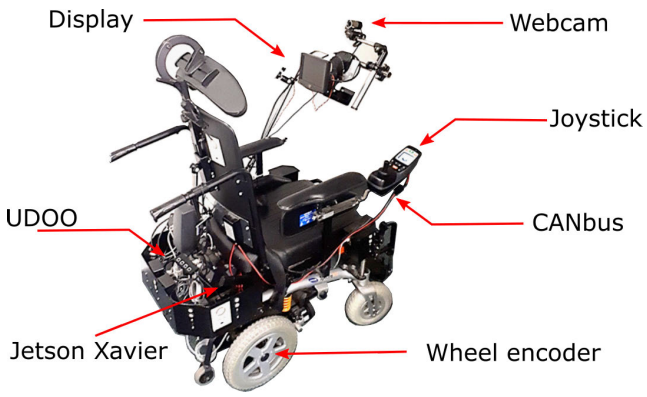

FIGURE 1. Our developed head-controlled robotic wheelchair.

interaction interfaces such as joystick control are not applicable for quadriplegics who have lost hand function. Due to the unique nature of quadriplegia, tracking head movements has drawn the attention of researchers as an alternative solution to operating a wheelchair. However, the literature reveals that this area is understudied, with only a few successful practical implementations of head gesture-based control.

Previous research can be broadly classified into two approaches: *invasive* and *non-invasive*. Invasive approaches require contact with the user's head, such as tilt and accelerometer sensors [2], [3], which can limit their movement range or cause discomfort. Non-invasive approaches, on the other hand, use computer vision techniques for image-based head pose estimation [4] or head gesture recognition [5], enabling contact-free operation of the wheelchair.

In this study, we present a novel *non-invasive* method that relies on visual head pose estimation for controlling a commercial Electric Powered Wheelchair (EPW) through head movements. Our approach improves upon existing methods by using a state-of-the-art neural network and fast, accurate facial landmark detection to perform robust face detection and head pose estimation. Furthermore, we have designed a calibration process that allows for customization of each individual's range of motion and a control logic that enables users to maintain full control over the wheelchair. Our system allows for continuous control, which is not present in other works.

Our main contributions include:

1) Designing a vision-based, non-intrusive, cost-efficient system for controlling a wheelchair through head movements, relying only on a simple web camera.
2) Improving upon existing methods by using a state-of-the-art neural network and fast, accurate facial landmark detection for robust face detection and head pose estimation.
3) Designing a calibration process for customization of each individual's range of motion and a control logic for maintaining full control over the wheelchair.
4) Allowing for continuous control, which is not present in other works.
5) Evaluating the system's effectiveness in a real-world scenario with healthy human participants.

The rest of this paper is organized as follows. Section II presents a literature review of existing head-controlled wheelchair methods. Section III describes our approach for estimating head position and controlling the wheelchair. Sections IV-A and IV provide details on the hardware setup of our wheelchair and the experimental protocol we followed, respectively. In Section V, we present trial results and a discussion of our findings. Lastly, Section VI summarizes our work and proposes future directions for building upon and further improving our novel system.

II. RELATED WORKS

Head-controlled wheelchairs are a key assistive technology for people suffering with motor disabilities in their four limbs. Following the distinction between *invasive* and *non-invasive* approaches made in section I, a broader classification of methods can be made between *sensor-based* and *vision-based*. In this chapter, we explore the most prominent sensor-based and vision-based head-controlled wheelchair studies.

A. SENSOR-BASED APPROACHES

Due to their simplicity and reliability, sensor-based techniques have been the focus of hands-free wheelchair control. Currently, the conventional method used by quadriplegic patients for wheelchair control is the sip-and-puff system [6], which allows basic control through a plastic tube mounted on the wheelchair. This system, even though low-cost and easy to use, has been reported to feel cumbersome, awkward and very slow. An alternative proposal to the sip-and-puff is the Tongue Drive System (TDS) [7], which detects the tongue motion by using a magnet and magnetic sensors. This system, however, requires the tongue to be pierced, which can be quite uncomfortable, and also allows a limited number of commands. Other methods that have been explored by the research community rely on tracking the head position, which has been achieved with a diversity of sensors including accelerometer, tilt sensors, touch switches, or ultrasounds.

As one of the first sensor-based head-controlled wheelchairs, [8] introduced a powered wheelchair steering technique with the aid of head movements, derived by ultrasonic range measurements. In this study, they have mapped the head orientation, estimated by two ultrasound sensors, into four discrete commands; right, left, moving forward and stop. Another contactless sensor-based approach, [9] explored the performance of a head-controlled EPW, where the motion was recorded by an array of four infrared LEDs and a camera. The number of infrared LEDs in the vision of the camera (installed at the back of the user's head, on the head rest) change according to the yaw angle of the user's face, and the discrete commands of turning right and left are derived from the number of LEDs that are within the camera's field of view. Reference [10] utilized an interface with mounted proximity infrared sensors, to track

the eyeball motion of a user and detect intentional blinks and eye motions, which are mapped to driving commands for the wheelchair. Using inertial sensors is another method of deriving the head orientation for controlling EPWs, and it is explored in several studies. Reference [11] is such an example, that used a MPU 6050 triple axis accelerometer and a gyroscope for monitoring the user's head motion and ultimately controlling a prototype EPW. However, no actual experiments verifying the effectiveness of the proposed method are presented. The authors embedded the accelerometer on the visor of a cap that needs to be worn by users. Similarly, [12] used an accelerometer to get the head position feedback before feeding that signal to an Arduino board to process the data and control a toy car, instead of a wheelchair. As an another example of sensor-based techniques, [13] used a gyroscope, attached on the user's head by a headband, for steering a real wheelchair. The proposed model has limited accuracy, whereas the accumulative error caused by the integration of the gyroscope output (known as the drift problem) has been considered negligible. Some other sensor-based approaches are presented in [2], [3], and [14], where tilt sensors were utilized for X and Y displacement detection, which was then translated to discrete wheelchair movement commands. The effectiveness of the tilt sensor-based approach in [3] was verified through trials run on Spinal Cord Injured (SCI) patients, by performing some basic tests like travelling in a straight line or measuring the braking distance after sending a stop command. Another direction of sensor-based methods in wheelchair control focuses on the use of the Electroencephalography (EEG) technique [15], [16], [17]. This approach, however, depends on using an electrode cap placed on the user's scalp for acquiring the brain signals, and faces important challenges, like a small signal-to-noise (SNR) ratio and multiple different noise sources which corrupt the main signal. It is currently considered very challenging to design and implement such a system, that is also reliable, accurate and flexible.

The methods presented above, usually come with a number of drawbacks. Installing the sensors, as well as maintaining them, due to the high probability of getting damaged, can incur high costs. Furthermore, the inconvenience, or the wearing discomfort, caused to the users by solutions such as the TDS, head switches, devices attached to the user's head etc., is as another important drawback. Finally, the majority of the existing approaches operate with a discrete set of moving commands, thus, limiting the amount of available control to the user.

B. VISION-BASED APPROACHES

Vision-based approaches for powered wheelchair control are much rarer compared to sensor-based approaches. The most widely explored vision-based approach is based on eye-tracking, where a number of different methods have been proposed for implementing it in a robust manner [18], [19], [20], [21]. Such methods typically work with capturing images of an eye, and using image processing techniques (e.g., Hough transform) to track the position of the eye pupil and then map it to a control direction for the wheelchair. One major shortcoming of such an approach is the limited reliability of tracking the eye pupil. Results can greatly vary depending on the quality of the image, the size or the colour of the pupil, the lighting conditions and the use of glasses or contact lenses. Furthermore, eye gaze control can be quite taxing to its user, since it requires constant eye movement and focus, which can cause dizziness or similar symptoms.

Despite eye-tracking, other methods utilizing cameras and computer vision algorithms have also been used on head-controlled wheelchairs, however, their number is limited. One such method is proposed in [5], where the head position is estimated with the aid of a Kinect and three landmarks on the head, by utilizing the optical flow technique. The estimated position is then mapped to four discrete commands for steering a wheelchair. However, the proposed method was only tested in controlling a pointer for following the path on a screen. Hu et al. [22] proposed a head gesture based interface for controlling a wheelchair, by using a combination of Viola-Jones [23], a well known face detection algorithm based on Haar features, and the Camshift algorithm for face detection and template matching for classifying the face posture. The reliability of these algorithms, though, is limited for such an application (Viola-Jones is not as effective detecting tilted or turned faces, while Camshift has poor accuracy). In a similar manner, [24] used a Haar cascade classifier for face and eyes detection, estimating their position to generate control commands for the wheelchair's motors. Notwithstanding the fast speed of the Haar classifier, it requires careful tuning, while it is known for high false positive detection rates and for being sensitive to the lighting conditions. No validation experiments were conducted for the aforementioned studies.

Other works propose using additional inputs, like mouth movements [25] or eye winking [26] along with the head position. However, this approach results in added complexity and discomfort using the system, while it allows more room for errors both from the system and the user side. Some studies including [25], [27], that have demonstrated their proposed systems in real world scenarios, provide implementations on laptops mounted on the wheelchair, which can harm the practical viability of a system that demands a low-power and mobile solution. Furthermore, in these works there is absence of subjective metrics and overall user experience evaluation, which is vital for assessing the actual usability of such systems.

A different type of approach is presented in [28], where the authors proposed an active vision approach, and instead of using a frontal camera pointing at the user's face they use an on-head camera. Halawani et. al used SIFT (Scale-Invariant Feature Transform) points to monitor head motion, and by comparing interest points extracted from consecutive image frames they obtain the movement direction in a discrete manner and steer the wheelchair in a real-world scenario. This method relies on identifying and matching stable and

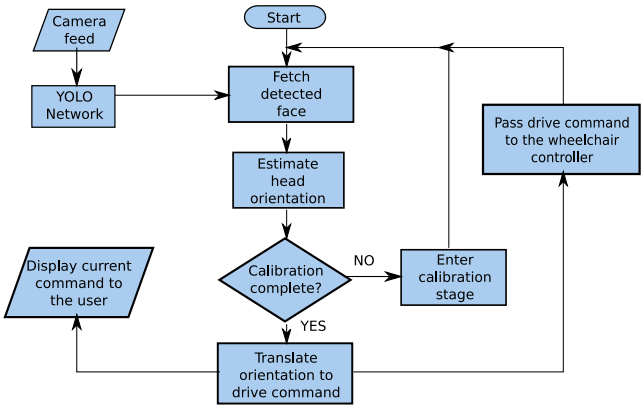

FIGURE 2. The system's flowchart.

repeatable points in different images, and even though it is a vision-based approach, it requires contact between the user and the camera (being installed on their head), which might cause inconvenience similar to sensor-based approaches.

C. OUR CONTRIBUTION

Exploring the literature on head-controlled wheelchairs reveals that very few of the proposed solutions have been put into real use. Namely, the sip-and-puff, TDS and eye-gaze technologies are the ones being used today by quadriplegic patients. Sip-and-puff and TDS are invasive methods, that can be burdensome to use for prolonged periods of time, while they offer limited control freedom. Eye-gaze, though vision-based and non-invasive, also does not allow fine control, while it can be unreliable and taxing to the user. Other works based on computer-vision are quite rare, and are usually sensitive to environmental conditions (including varying illumination, indoor and outdoor environments, cluttered backgrounds, and shadows [29]), or their effectiveness has not been explored in depth by being applied to a real system and tested with human subjects.

In this study, we present a vision-based, non-intrusive, cost-efficient system for controlling a wheelchair via head movements, only relying on a simple web camera. We have designed a system that robustly performs face detection and head pose estimation, improving upon similar existing methods [22], [24], by combining a state-of-the-art neural network and a fast and accurate facial landmark detector. We have also designed a calibration process that allows customization to each individual's range of motion and a control logic which allows users to maintain full control over a powered wheelchair. Furthermore, the control can be done in a continuous manner, something that is not present in other works. The system has been deployed on a commercial wheelchair and its effectiveness has been evaluated on a real world scenario with healthy human participants.

III. METHODOLOGY

A robust head-controlled wheelchair requires two important elements; a reliable head pose estimation algorithm and a robust translation of the orientation to commands for the robotic wheelchair. Therefore, our method consists of two main modules, one for estimating the head orientation (pitch and yaw), and another one for translating the derived orientation to velocity commands, before passing them to the control module of the EPW. For the head pose estimation step, we propose the use of "YOLO" (You Only Look Once), a widely-used Convolutional Neural Network (CNN), along with a facial landmark detector, where the head pose would be calculated with respect to the output of these two blocks (see next section for more info). For mapping the output of the head pose estimation to moving commands for the robotic wheelchair, we experiment both with discrete control commands (predetermined velocity values for turning), as well as continuous control commands (turning is a linear function of the head's yaw). A detailed explanation will be provided in the rest of the chapter, where we present the methodology behind our approach.

A. HEAD POSE ESTIMATION

For estimating the head orientation, in the pitch and yaw dimensions, we utilize two modules combining machine learning and more traditional computer vision techniques. The first module is responsible for detecting the head of a person within an image, whereas the second one is used to approximate the orientation of the detected head. For head detection we utilized the well-known YOLOv3 network [30], which is a fast and efficient Fully Convolutional Neural Network (FCNN), capable of detecting multiple objects in almost real-time. YOLO uses a feature pyramid network to detect objects at different scales and resolutions. This, along with data augmentations during training, makes YOLO more robust to environmental factors, such as different lighting conditions and levels of blur, compared to other face detection methods, like Viola Jones.

To improve performance in detecting faces on the wheelchair's onboard processor, we used mini-YOLOv3, a smaller version of the full YOLOv3 network that was retrained for this specific task. Mini-YOLOv3 was chosen for its smaller size and faster frames per second (fps) compared to the full YOLOv3 network. Despite its smaller size, mini-YOLOv3 maintains comparable accuracy to the original network, and is particularly effective in detecting the closest face to the camera. Other studies have also demonstrated the effectiveness of mini-YOLOv3 as a real-time object detector for embedded applications [31]. The implementation used, "DarknetROS" [32] was chosen because it is compatible with ROS (Robot Operating System), which serves as the backbone of the overall system. More information about ROS is provided in Section IV-A1.

The detected face is then passed on to the second module, which uses computer vision techniques in order to locate the facial features contained in the image. For this, we used the *facial landmark detector* included in the "Dlib" library, which is an implementation of the work done in [33], that

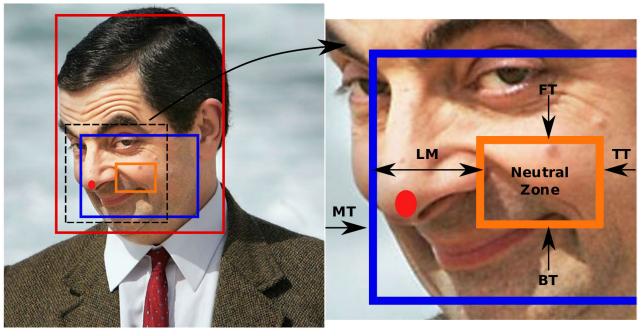

FIGURE 3. **Left - The detected face (red bounding box) and the calibration boundaries, against which the nose tip position (red circle) is checked. The orange bounding box indicates the limits of the neutral zone, and the blue the limits of the maximum motion in both directions, as calibrated by the user (see Sec. III-B) Right - FT: The threshold for initiating forward movement BT: The threshold for initiating backward movement TT: The threshold for initiating turning LM: The interval at which the horizontal nose tip position is linearly mapped to angular velocities (only in continuous mode) MT: The threshold beyond which the maximum allowed turning speed is set.**

learns an ensemble of randomized regression trees to detect landmarks on a face image. The particular method was chosen for its proved effectiveness and high speed [34], vital for achieving real-time processing times. From those features, we choose to locate the tip of the nose, the position of which provides a good approximation of the head's orientation. The nose position is given in x and y coordinates of the given frame, but since the bounding box of the face is of variant size (depending on the distance of the face to the camera), the head orientation is calculated as percentages of the nose's location in the image relative to the current frame's size (rows x columns). Naturally, the vertical coordinate changes along with the pitch movement of the head, whereas the horizontal with the yaw movement as shown in Figure 4.

1) SMOOTHENING THE INPUT

Here, it is important to mention that instead of directly using the current pitch and yaw values for moving the EPW, a moving average is computed using the *sliding window method* for the past k frames. This makes the implementation much more robust for two reasons: Firstly, it prevents the translation of noisy estimates to immediate driving commands, and secondly, it allows space for the user to make errors, like for example sudden tweaks of the head, without instantaneously altering their driving course. Of course, the size of the window is adjustable and dependent both on the hardware (fps of the head detection) and also the preference/capability of the individual user, and therefore needs to be tuned accordingly. For example, given the last k pitch measurements, the current smoothed pitch value would be given by: $\bar{p}_n = \frac{1}{k}\sum_{i=1}^{k} p_i$

For the next moving average calculation, and in order to save processing time, the calculation can be simplified by reusing the previous moving average. A new pitch value p_{n+1} comes into the window, whereas the oldest value p_{n-k+1} drops out, thus we get: $\bar{p}_{n+1} = \bar{p}_n + \frac{1}{k}(p_{n+1} - p_{n-k+1})$.

B. HEAD POSE TO CONTROL OF THE ROBOTIC WHEELCHAIR

After the extraction of the values corresponding to the pitch and the yaw of the head, we apply a control script which is responsible for translating those values to velocity commands, as well as implementing the control logic to operate the EPW. Here, it is important to mention that in the case where either the camera loses the user's face, or in the exceptional case that there is no valid face detection or pose estimate, no control command will be issued to the wheelchair, bringing it to a halt.

A valid head pose can be translated in either a *discrete* or a *continuous* manner, where in the first case the discrete mode (DM) maps the pitch values to three regions (''moving forward'', ''moving backward'', ''neutral''), and likewise the yaw values to three regions (''turning right'', ''turning left'', ''neutral/inactive''). In the second case, the continuous mode (CM) retains the same mapping for the pitch, but uses a linear mapping for the yaw values to angular velocities. For a differential drive system the linear velocity and the angular velocity can be expressed as follows:

$$v_x = \frac{v_R + v_L}{2} \quad \omega = \frac{v_R - v_L}{l}, \tag{1}$$

where v_x is the platform body's linear velocity, ω is its angular velocity, $v_{R,L}$ are the drive wheel velocities (right and left respectively) and l is the axial distance between the two drive wheels.

Below, we further explain both modes and the control flow of our system, which is also summarized in Figure 2.

1) DISCRETE CONTROL

Before sending commands to move the robotic wheelchair, a calibration phase needs to first take place. In the calibration phase, the user is given some fixed time to set their ''neutral zone'', which is defined by the maximum and minimum values of the pitch and yaw estimates, when the user moves their head very slightly in all directions, while seated in their neutral/comfortable straight position. The neutral zone can be visualized as a virtual box around the user's nose, where, while the nose remains there, no velocity commands are being sent to the EPW.

After the calibration is complete, we enter the driving phase, during which the current orientation is checked relative to the neutral zone. When the pitch value exceeds the upper bound of the neutral zone in the vertical direction, the linear velocity v_x of the EPW is set to a predefined positive value, and remains so as long as the vertical position does not exceed the lower bound of the neutral zone. If the latter happens, then the linear velocity is set back to zero, unless it remains there for a set amount of time, in which case ''reverse'' is enabled, setting the linear speed to a predefined negative value. Reverse can then be cancelled by again exceeding the upper vertical bound.

Similarly, we set the angular speed ω of the EPW to a predefined positive or negative value, when the yaw value

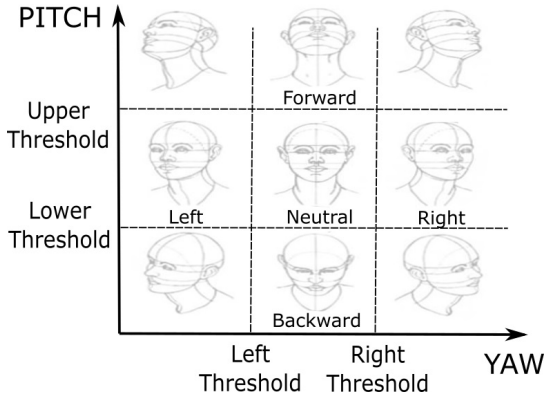

(a) Mapping of head position to moving commands.

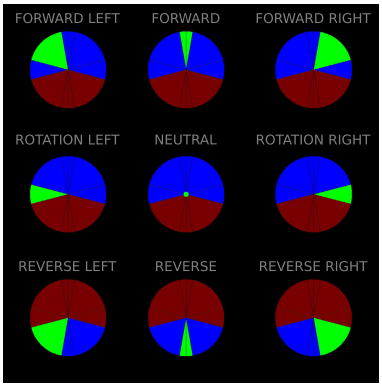

(b) The moving commands displayed as a virtual joystick to the user.

FIGURE 4. Visualization of the head control process.

exceeds the right or left boundaries (in the horizontal direction) of the neutral zone respectively. The difference when turning, is that the head position needs to remain either right or left, and beyond the neutral thresholds, to maintain a non-zero angular speed. This is done purposely to make turning more responsive, as well as easily cancelable simply by moving the head back to the neutral position. When the linear velocity is set to zero, the user can turn their head right or left to make the EPW rotate on the spot towards the desired direction.

2) CONTINUOUS CONTROL

With "continuous control" we refer to producing continuous, instead of constant values, for controlling the angular speed of the EPW. In this mode, the linear speed again remains constant as previously described. The control process for continuous mapping is similar to the discrete one, with two important differences. Firstly, we add an additional step in the calibration phase, where the user has to also set their maximum (comfortable) range of motion in the yaw direction, in order to obtain another boundary in the horizontal direction outside the neutral one. Given this additional boundary, we can now map any right or left head movement that exceeds the neutral zone, to a continuous value between a minimum one (a fraction of the maximum angular speed, $\omega_{min} = \alpha \cdot \omega_{max}, \alpha \in [0, 1)$), up to the maximum allowed one (ω_{max}) when the head is at (or exceeds) the edge of the outer boundary. For example, in the case of a right turn of the head, and given the calibrated right neutral boundary nb_r, the far right boundary b_r, and the estimated *yaw* value y, the angular velocity mapping is described below:

$$\omega(y) = \begin{cases} 0, \text{ if } y \leq nb_r \\ \omega_{min} + \dfrac{\omega_{max} - \omega_{min}}{b_r - nb_r}(y - nb_r), \\ \qquad \text{if } y > nb_r \text{ and } y \leq b_r \\ \omega_{max}, \text{ otherwise.} \end{cases} \tag{2}$$

The same calculation also applies for a left turn, but checked in respect to the left calibrated boundaries and mapped to negative angular speeds. A graphic depiction of the above process is provided in Figure 3.

IV. EXPERIMENTAL TRIALS

A. WHEELCHAIR SETUP

In order to test the performance of both approaches, we run a set of experimental tests on a real EPW, in which the behavior of users, models and wheelchair has been extensively explored.

1) WHEELCHAIR COMPONENTS

The wheelchair that was used for our experiment is a Spectra XTR2 model (Figure 1), which was modified accordingly for compatibility with the Robot Operating System (ROS), a framework that was chosen to enable interconnectivity between the different components of the system. Programs that use the ROS framework are termed as "ROS Nodes", and multiple nodes can be running in parallel and independently. Nodes can communicate between them through the use of "topics" that carry messages, and by using the standard TCP/IP protocol. In our case, each of the main processes of the system (i.e., head detection, head pose estimation, head pose to EPW commands) was written as a ROS node, to be able to receive and/or pass messages from/to ROS topics. The sensors of the system, as well as the EPW's controller, also make use of the same framework (e.g., the web camera passing the images it captures to a ROS topic or the controller receiving commands as messages from another ROS topic).

The basic processing unit of the EPW is a UDOO board, which is connected to the main sensors of the wheelchair (e.g., encoders), as well as the control unit through the joystick controller (a DX2-REM550/551 Advanced Joystick Remote model). A NVIDIA Jetson Xavier board was also connected to the UDOO, via Ethernet to allow ROS message-passing, and in order to execute the higher level, computer

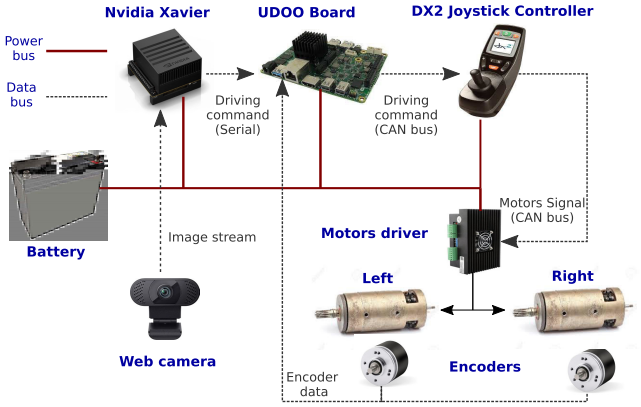

FIGURE 5. The wheelchair's hardware setup.

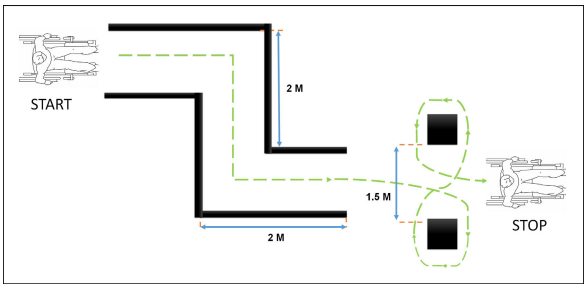

FIGURE 6. The experimental route layout.

vision tasks. A simple web camera (any camera that can provide images with a resolution higher than 416×416 pixels, which is the standard input resolution for YOLOv3, is acceptable) is streaming the captured images to the Xavier, which processes them as described in Section III and produces a velocity command. The resulting command is in turn passed to the UDOO board and ultimately to the EPW's control module to move the wheelchair. The hardware layout, along with connections between the components, is presented in Figure 5, while a visualization of the mapping of head movements to control commands, as well as the virtual joystick that is displayed as feedback to the user, are shown in Figure 4.

2) ENCODERS

A pair of incremental rotary encoders was also utilized (one encoder per driving wheel), in order to calculate odometry data (defined as the use of motion sensors to determine the robot's change in position over time) and be able to visualize the trajectory executed by the wheelchair throughout the trials. Below, we present the equations that were used, based on the differential drive kinematics, in order to derive the velocity and the displacement of the EPW via the encoder information.

For a full revolution of the wheel, the encoder performs a certain number of "ticks" (t_{pr}). Given that information, along with the radius (r) of our drive wheels, we can then calculate the distance that corresponds to each of those "ticks" as

$$mms_{per.tick} = \frac{2\pi r}{t_{pr}}. \tag{3}$$

By measuring the difference in "ticks" between two consecutive measurements of an encoder (d_{ticks}), and from the kinematic equations that describe a differential drive platform (shown in Eq. 1), it is possible to calculate the robot's displacement and change in heading from the following equations:

$$d_{xy} = \frac{mms_{per.tick}}{2} \cdot (d_{ticks.right} + d_{ticks.left}) \tag{4}$$

and

$$d_{th} = \frac{mms_{per.tick}}{l} \cdot (d_{ticks.right} - d_{ticks.left}). \tag{5}$$

B. EXPERIMENTAL PROTOCOL

In this study, we recruited 14 healthy people to participate in the experimental tests. We run three experiments per participant, where they were asked to navigate the wheelchair through the designed track (as shown in Figure 6) in the following modes: (i) using the manufacturer's standard joystick interface (ii) using the head-control method in DM (iii) using the head-control in CM. The age of the participants ranged between 21 and 56 years old. During the experiments, an emergency button was connected to the wheelchair for safety reasons. This button would disconnect the main power in case of an emergency. The participants were also instructed to use the joystick (which would override the remote head commands) only in the event of a potential collision, but not for correcting the trajectory of the wheelchair. Before each trial, every participant was provided with three opportunities to calibrate the system.

The participants were given up to 15 minutes to familiarize themselves with the setup as well as the driving behaviour of the EPW, and also a 2 minute break between the different experimental rounds, in order to minimize the effect of tiredness or any other unwanted factors. An interview was conducted after the trial to gauge the participant's satisfaction with the system and to collect some subjective measurements. The participants were asked to provide a number between one and five (1-5), stating their experience with using a powered wheelchair.[1]

For the sake of performance evaluation, the *trajectory*, *number of collisions*, *travelling time* and *travelling distance* were recorded throughout the trial runs. The number of collisions, as well as the travelling time, were recorded by the researchers overviewing the trials, whereas the trajectory and the travelling distance were extracted from the odometry data derived from the pair of encoders installed at the EPW's wheels (see Sec. IV-A2). The performance of the participants

[1]Some of the participants were members of the research teams working in the area of assistive technologies, therefore having experience with wheelchairs, despite being non-disabled.

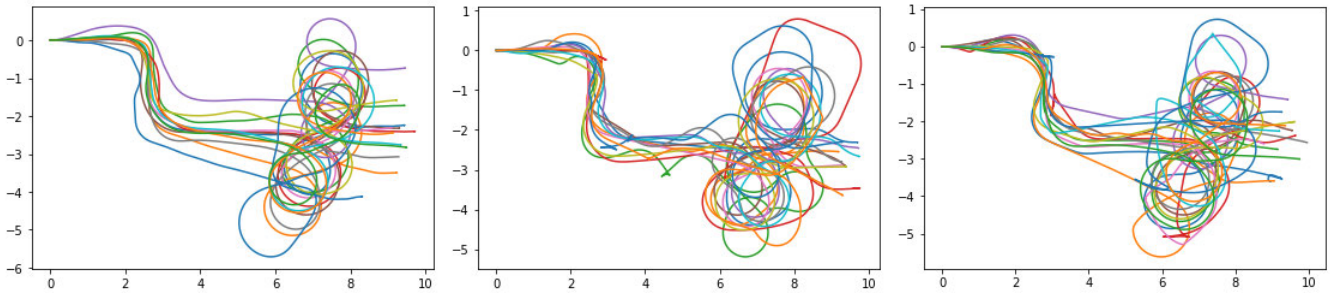

(a) Joystick (b) Head control in DM. (c) Head control in CM.

FIGURE 7. The trial trajectories as recorded from the odometry.

TABLE 1. Participant trial results in the three driving modes.

Mode	Statistics					
	Distance (m)		Time (s)		Collisions*	
	Mean	Std	Mean	Std	Mean	Std
Joystick	21.2	1.31	67	0.08	0	0
DM	23.4	2.73	92	0.29	2.84	2.07
CM	23.2	2.13	81	0.23	2.5	2.44

* As collision we regard any contact of the wheelchair with obstacles, plus any momentarily intervention with the standard joystick controller, in cases where users felt they were not in control or panicked

has been evaluated qualitatively and quantitatively and is discussed in the following chapter.

V. RESULTS AND DISCUSSION

We have evaluated the participants' performance in each of the three modes with a set of evaluation metrics as:

- Mean and standard deviation of traveling time
- Mean and standard deviation of traveling distance
- Number of collisions
- A number of subjective measurements inspired by the Nasa Task Load Index [35] (*only in head-control mode*)

The summary statistics of the travelling distance, travelling time and the number of collision are presented in Table 1. For gaining a better insight of the participants' performance in each mode, the travelling trajectories, constructed from the recorded odometry, are also presented in Figure 7.

A. ANALYSIS OF THE RESULTS

For the 14 participants a total of 28 distinct runs were conducted using our head control system (2 modes per participant) and another 14 using the standard joystick interface, making a total of 42 runs. For a fair comparison, the commands issued from the joystick were limited to match the maximum allowed velocities of the head control mode. Out of the 28 head-controlled runs, 27 were successfully completed, whereas there was 1 case where the participant could not complete the trial, due to poor calibration of the system (''reverse'' could not be activated). As stated in the study protocol (Section IV-B), each participant had up to three tries to successfully calibrate the system.

Comparing the *discrete* versus the *continuous* translation of the head pose estimation to moving commands, our observation revealed that the *continuous* performed slightly better, in terms of completion times, but also shorter trajectories and smaller number of collisions. This can also be verified visually by comparing the resulting trajectories between Figure 7b (*discrete*) and Figure 7c (*continuous*). This result was expected, and is accounted to the finer control (or greater resolution) for turning that the *continuous* implementation allows. However, our observations revealed that the CM performed better for some participants, while for others the DM was the better option, especially for the ones who had no prior experience with using an EPW. To explore this observation further, we split the completion times of the participants into two groups; one with the absolute amateurs in wheelchair driving (1), and the other with the rest of the participants that had little to much experience (2-5). On those groups we performed a two sample t-test (Welch's t-test, alpha level of 0.05) and found a statistical significance in completion times when using the CM ($p = 0.045$). On the other hand, a significant trend was not found for the respective test in the DM ($p = 0.41$).

Furthermore, we run a correlation analysis between the participants' self-reported wheelchair experience and the users' performance in terms of completion times. The metric that was used was the *Pearsons correlation coefficient* (PCC) [36], which is an interpretable measure of linear correlation between two sets of data. We obtained the scores of -0.19 and -0.46 for the *discrete* and *continuous* mode respectively. The negative correlation shows an inverse relationship between completion times and experience (the more experience the shorter the completion times), with the correlation in the DM being small, and in the CM being moderately high. This is an indication, that having no prior experience with driving a wheelchair does not greatly affect the performance in the DM, but does affect the performance in the CM, making it possibly a better option for experienced users. It is logical that the DM works better for inexperienced users because it allows more room for mistakes. In contrast, the CM may be more difficult to use because it is more sensitive to horizontal head movements, but it also has the potential

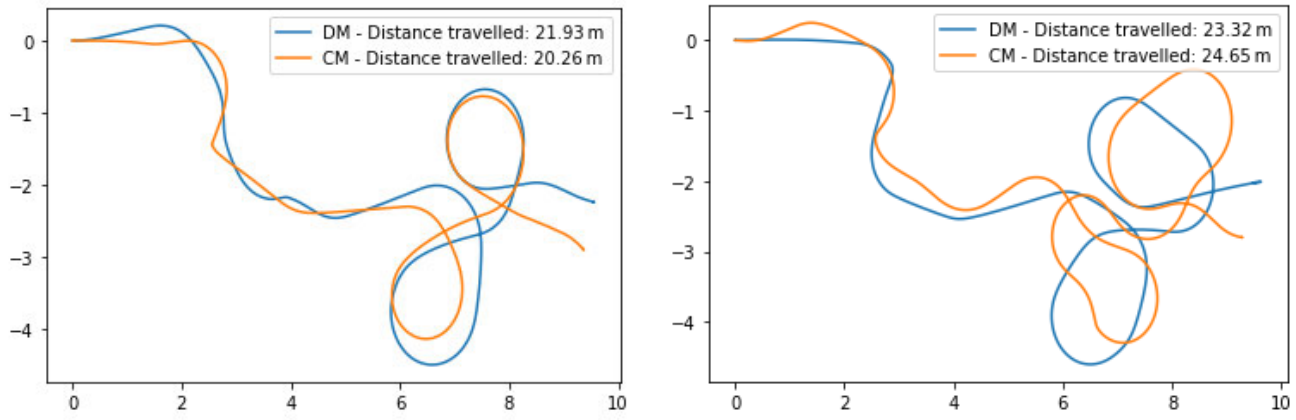

(a) Recorded trajectories of an experienced (5) user.

(b) Recorded trajectories of an inexperienced (1) user.

FIGURE 8. Trajectories of an experienced vs an inexperienced user of head control in DM and CM. The experienced user takes better advantage of the CM, managing to perform sharper and more accurate turns compared to the DM. On the other hand, the inexperienced user has a more "shaky" performance in the CM, thus performing worse than the DM which has a more predictable behaviour.

to perform better than the DM since it allows for finer control. Figure. 8 shows an example of recorded trajectories by an experienced and an inexperienced user, which highlight the results presented above.

To compare the performance between the joystick and head-control modes, we conducted pairwise statistical comparisons using the completion times of the participants. We first compared the joystick and head-control in discrete mode using a two-sample t-test (Welch's t-test, alpha level of 0.05). The analysis showed a significant difference between the two modes ($t(24.67) = -6.04, p < 0.001$), with the joystick mode having significantly shorter completion times. We then compared the joystick and head-control in continuous mode using the same statistical test. The results revealed a significant difference between the two modes ($t(18.12) = -4.58, p < 0.001$), with the joystick mode again having significantly shorter completion times. Furthermore, in the DM we have an increase of 10.4% for the trajectory length compared to the joystick, whereas in the CM we have an increase of 9.4%. These findings suggest that the joystick mode offers better performance than the head-control modes, which is in line with our expectations due to the easier use and better accuracy of the joystick. However, it is worth noting that the head-control modes were not significantly inferior to the joystick mode, indicating that they could serve as a viable alternative for individuals who struggle with operating a joystick.

Looking at the statistics of the collisions that occurred during the head-control runs, we observe high standard deviations (2.07 in DM, 2.44 in CM). The people that got accustomed to the system, drove with a good level of control and had no to very few collisions. On the other hand, some participants were unable to adjust to the system within the allotted time of 15 minutes. This was due to either failing to calibrate the system properly or getting nervous during the trials. As a result, they lost control and crashed multiple times before completing the course.

B. SUBJECTIVE MEASUREMENTS

Despite the objective measurements that were recorded and analyzed, we are also interested in evaluating the participants' experience of using our system. For that purpose, we utilized measurements of the NASA Task Load Index (NASA-TLX), a widely used, multidimensional assessment tool that rates perceived workload in order to assess a system's effectiveness. More specifically, the measurements that we used are:

- *Mental demand* - How mentally demanding was the task?
- *Physical demand* - How physically demanding was the task?
- *Performance* - How successful were you in accomplishing what you were asked to do?
- *Frustration* - How insecure, discouraged, irritated, stressed, or annoyed were you?

The participants were asked to provide their own evaluation on the above categories on a scale of 1-20, 1 being "Very low" and 20 being "Very high", in order to assess their overall experience with using our head control system (not differentiating between the two modes). The results are presented in Table 2.

Overall, we can see that the participants reported a low physical demand (mean of 5.6), but higher mental demand and frustration (9.3 and 7.1 respectively), although still reasonably low. The physical demand has a low standard deviation (3.9), indicating agreement of the participants, whereas the deviation increases when it comes to the mental demand (5.2) and frustration (5.5), showing that the task was less taxing for some of the participants, but more taxing to others. This result also agrees with our observation of the previous section, since running a correlation analysis between the experience and the frustration and the mental demand of the participants resulted in a PCC of -0.34 and -0.29 respectively, indicating an effect of the experience on the perceived effort of the users. On the contrary, a PCC of -0.13 between

TABLE 2. Participants' subjective measurements results.

Metrics	Statistics		
	Mean	Std	Median
Mental Demand(1-20)	9.3	5.2	8
Physical Demand(1-20)	5.6	3.9	5
Performance(1-20)	15.0	2.8	15
Frustration(1-20)	7.1	5.5	5
Wheelchair Experience(1-5)	2.4	1.5	2.0

experience and physical demand shows a weak correlation of how the users' physical comfort was affected by experience. Additionally, calculating the PCC between mental demand and the number of collisions, results in 0.04 in DM and 0.44 in CM. These results reveal that the mental demand that was experienced by the participants was mostly accounted to the CM, rather than the DM, for which the correlation was negligible. On the other hand, the participants reported a high evaluation of their own performance (15.0), with the lowest deviation (2.8), implying that overall they felt confident with their ability of using our system successfully for the task they were given.

C. DISCUSSION

The results of the conducted trials showed that the non-disabled participants were able to successfully use the head-controlled system and complete the designed track, demonstrating the effectiveness of the system in matching the use of a standard joystick controller. Although the joystick proved to be a faster and more accurate means of control, the head-controlled system was not far behind, especially given the difficulty difference between the tasks and the limited experience of the participants with the head-controlled system.

In terms of the head-control mode, the comparison between the continuous and discrete modes showed that the continuous mode performed slightly better in terms of smoother and more accurate control, particularly for users with more experience in driving a wheelchair. However, this was not the case for all participants, and the discrete mode may be a better option for inexperienced users as it provides more room for error. The statistical comparisons performed in the study support these findings, with a significant difference in completion times between the continuous and discrete mode for users with some experience in wheelchair driving, and a moderate negative correlation between completion time and experience for the continuous mode.

Furthermore, the comparison with the joystick control mode revealed that head-control with either the continuous or discrete mode can produce comparable results, albeit with slightly longer completion times and trajectory lengths. However, the absence of collisions during joystick runs indicates that joystick control remains the most reliable and safe option.

Calibration of the head-controlled system was found to be an essential factor in successful runs, with good calibration allowing full control of the wheelchair within a reasonable range of head movement. More work will need to be done on this aspect to ensure more consistent calibration results, as for example adding more visual cues to guide the user, while an additional step that allows users to set their desired velocity ranges would provide better customization. Changes in user posture, which can occur due to factors such as fatigue or differences in terrain, can have a considerable impact on the accuracy of the calibrated system during use. To address this, a dynamic re-calibration process during driving would be a valuable addition, allowing the system to adapt to such changes, leading to a more comprehensive and resilient solution.

The reports of the participants revealed that the most demanding part of the experiment was the calibration/training part, where they needed to familiarize themselves with the system and build confidence in using it. However, given the low reported physical demand and the potential reduction of mental demand and frustration with more experience, the head-controlled system may be a realistic and appropriate option for usage by actual wheelchair users. Further research and experimentation will need to be conducted to verify this hypothesis.

In conclusion, the choice between the continuous and discrete mode of head-control for an electric powered wheelchair depends on the user's level of experience in wheelchair driving. The continuous mode offers finer control, which leads to better performance in terms of completion time, trajectory length, and collisions for experienced users. However, the discrete mode may be a better option for inexperienced users as it provides more room for error. It is essential to consider the user's experience and training in choosing the appropriate control mode to optimize the performance and safety of electric powered wheelchair driving.

VI. CONCLUDING REMARKS

The purpose of our study was to develop a vision-based head-controlled wheelchair and evaluate its performance in real-world experiments. We combined a deep-CNN for detecting the face of interest in a stream of camera frames with a facial landmark detector to estimate the head pose, which was then translated into moving commands for a robotic wheelchair. We conducted experiments that required participants to complete a routing task, and both quantitative and qualitative analyses were performed to evaluate the system's performance and the participants' experience.

The results showed that our system had a 96% success rate in completing the task and was a viable alternative to the conventional joystick interface. Participants reported feeling confident in their performance with the system while experiencing relatively low mental and physical load. Our findings revealed the operational characteristics of the system and identified factors contributing to its performance, including control frequency, calibration process, and user experience.

The control frequency of the system was addressed by achieving an overall frequency of around 30Hz, which proved adequate to smoothly control our EPW. The use of

mini-YOLOv3 played a crucial role in this, as when using the full YOLOv3 instead, we only achieved a frequency of ∼5Hz, which significantly affected the final performance of the system at a preliminary testing stage. The calibration process was found to be sensitive and not very intuitive for some users, however, building more experience with the system makes the process easier and more effective over time, which in some cases was not possible to be achieved within the short training time provided in the experiment. We are confident that adding more visual cues to guide the calibration process will greatly improve its robustness, and therefore, the driving performance.

Reverse movement is supported by our design, but it should be combined with the feed of a rear-view camera to make it fully usable. Alternative filtering methods could be used to translate head position to velocity commands, and combining the output of our system with a collision avoidance module would ensure safe navigation.

Our study has shown promising results for the use of a vision-based head-controlled wheelchair, but further testing is needed with real powered wheelchair users, especially quadriplegics, in a clinical trial setting to verify its effectiveness for the target population. Overall, our system has the potential to improve the mobility and independence of wheelchair users, and we believe that our findings will contribute to the development of more effective and customizable systems in the future.

REFERENCES

[1] *Facts and Figures at a Glance*, Nat. Spinal Cord Injury Stat. Center, Univ. Alabama Birmingham, Birmingham, AL, USA, 2016.

[2] S. Kumar, N. Dheeraj, and S. Kumar, "Design and development of head motion controlled wheelchair," *Int. J. Adv. Eng. Technol.*, vol. 8, no. 5, pp. 816–822, 2015.

[3] Y.-L. Chen, S.-C. Chen, W.-L. Chen, and J.-F. Lin, "A head orientated wheelchair for people with disabilities," *Disability Rehabil.*, vol. 25, no. 6, pp. 249–253, Jan. 2003.

[4] S. M. Bafti, S. Chatzidimitriadis, and K. Sirlantzis, "Cross-domain multitask model for head detection and facial attribute estimation," *IEEE Access*, vol. 10, pp. 54703–54712, 2022.

[5] F. A. Kondori, S. Yousefi, L. Liu, and H. Li, "Head operated electric wheelchair," in *Proc. Southwest Symp. Image Anal. Interpretation*, Apr. 2014, pp. 53–56.

[6] I. Mougharbel, R. El-Hajj, H. Ghamlouch, and E. Monacelli, "Comparative study on different adaptation approaches concerning a sip and puff controller for a powered wheelchair," in *Proc. Sci. Inf. Conf.*, 2013, pp. 597–603.

[7] J. Kim, H. Park, J. Bruce, D. Rowles, J. Holbrook, B. Nardone, D. P. West, A. Laumann, E. J. Roth, and M. Ghovanloo, "Assessment of the tongue-drive system using a computer, a smartphone, and a powered-wheelchair by people with tetraplegia," *IEEE Trans. Neural Syst. Rehabil. Eng.*, vol. 24, no. 1, pp. 68–78, Jan. 2016.

[8] J. M. Ford and S. J. Sheredos, "Ultrasonic head controller for powered wheelchairs," *J. Rehabil. Res. Develop.*, vol. 32, no. 3, pp. 280–284, 1995.

[9] D. J. Kupetz, S. A. Wentzell, and B. F. BuSha, "Head motion controlled power wheelchair," in *Proc. IEEE 36th Annu. Northeast Bioeng. Conf. (NEBEC)*, Mar. 2010, pp. 2–3.

[10] M. Jain, S. Puri, and S. Unishree, "Eyeball motion controlled wheelchair using IR sensors," *Int. J. Comput. Inf. Engineer*, vol. 9, no. 4, pp. 1012–1015, 2015.

[11] J. W. Machangpa and T. S. Chingtham, "Head gesture controlled wheelchair for quadriplegic patients," *Proc. Comput. Sci.*, vol. 132, pp. 342–351, 2018, doi: 10.1016/j.procs.2018.05.189.

[12] S. Prasad, D. Sakpal, P. Rakhe, and S. Rawool, "Head-motion controlled wheelchair," in *Proc. 2nd IEEE Int. Conf. Recent Trends Electron., Inf. Commun. Technol. (RTEICT)*, May 2017, pp. 1636–1640.

[13] M. Bureau, J. M. Azkoitia, G. Ezmendi, I. Manterola, H. Zabaleta, M. Perez, and J. Medina, "Non-invasive, wireless and universal interface for the control of peripheral devices by means of head movements," in *Proc. IEEE 10th Int. Conf. Rehabil. Robot.*, Jun. 2007, pp. 124–131.

[14] S.-H. Chen, Y.-L. Chen, T.-S. Kuo, C.-Y. Chu, and C.-N. Hung, "M3S-based electrical wheelchair with head-controlled device," in *Proc. Int. Conf. IEEE Eng. Med. Biol. Soc.*, Aug. 2006, pp. 4917–4920.

[15] E. J. Rechy-Ramirez and H. Hu, "An electric wheelchair controlled by head movements and facial expressions: Uni-modal, bi-modal, and fuzzy bi-modal modes," in *Handbook of Research on Investigations in Artificial Life Research and Development*. IGI Global, 2018, pp. 1–30.

[16] Z. T. Al-Qaysi, B. B. Zaidan, A. A. Zaidan, and M. S. Suzani, "A review of disability EEG based wheelchair control system: Coherent taxonomy, open challenges and recommendations," *Comput. Methods Programs Biomed.*, vol. 164, pp. 221–237, Oct. 2018, doi: 10.1016/j.cmpb.2018.06.012.

[17] I. A. Mirza, A. Tripathy, S. Chopra, M. D'Sa, K. Rajagopalan, A. D'Souza, and N. Sharma, "Mind-controlled wheelchair using an EEG headset and Arduino microcontroller," in *Proc. Int. Conf. Technol. Sustain. Develop. (ICTSD)*, Feb. 2015, pp. 1–5.

[18] F. B. Taher, N. B. Amor, and M. Jallouli, "A multimodal wheelchair control system based on EEG signals and eye tracking fusion," in *Proc. Int. Symp. Innov. Intell. Syst. Appl. (INISTA)*, Sep. 2015, pp. 1–8.

[19] P. S. Gajwani and S. A. Chhabria, "Eye motion tracking for wheelchair control," *Int. J. Inf. Technol. Knowl. Manag.*, vol. 2, no. 2, pp. 185–187, 2010.

[20] C. S. Lin, C. W. Ho, W. C. Chen, C. C. Chiu, and M. S. Yeh, "Powered wheelchair controlled by eye-tracking system," *Optica Applicata*, vol. 36, nos. 2–3, pp. 401–412, 2006.

[21] N. Wanluk, S. Visitsattapongse, A. Juhong, and C. Pintavirooj, "Smart wheelchair based on eye tracking," in *Proc. 9th Biomed. Eng. Int. Conf. (BMEiCON)*, Dec. 2016, pp. 1–4.

[22] P. Jia, H. H. Hu, T. Lu, and K. Yuan, "Head gesture recognition for hands-free control of an intelligent wheelchair," *Ind. Robot, Int. J.*, vol. 34, no. 1, pp. 60–68, Jan. 2007.

[23] P. Viola and M. Jones, "Rapid object detection using a boosted cascade of simple features," in *Proc. IEEE Comput. Soc. Conf. Comput. Vis. Pattern Recognit. (CVPR)*, Dec. 2001, pp. 511–518.

[24] R. Solea, A. Margarit, D. Cernega, and A. Serbencu, "Head movement control of powered wheelchair," in *Proc. 23rd Int. Conf. Syst. Theory, Control Comput. (ICSTCC)*, Oct. 2019, pp. 632–637.

[25] J. S. Ju, Y. Shin, and E. Y. Kim, "Vision based interface system for hands free control of an intelligent wheelchair," *J. NeuroEng. Rehabil.*, vol. 6, no. 1, pp. 1–17, Dec. 2009.

[26] L. M. Bergasa, M. Mazo, A. Gardel, R. Barea, and L. Boquete, "Commands generation by face movements applied to the guidance of a wheelchair for handicapped people," in *Proc. 15th Int. Conf. Pattern Recognit. (ICPR)*, 2000, pp. 660–663.

[27] E. Perez, C. Soria, O. Nasisi, T. F. Bastos, and V. Mut, "Robotic wheelchair controlled through a vision-based interface," *Robotica*, vol. 30, no. 5, pp. 691–708, Sep. 2012.

[28] A. Halawani, S. U. Réhman, H. Li, and A. Anani, "Active vision for controlling an electric wheelchair," *Intell. Service Robot.*, vol. 5, no. 2, pp. 89–98, Apr. 2012.

[29] H. G. M. T. Yashoda, A. M. S. Piumal, P. G. S. P. Polgahapitiya, M. M. M. Mubeen, M. A. V. J. Muthugala, and A. G. B. P. Jayasekara, "Design and development of a smart wheelchair with multiple control interfaces," in *Proc. Moratuwa Eng. Res. Conf. (MERCon)*, May 2018, pp. 324–329.

[30] J. Redmon, S. Divvala, R. Girshick, and A. Farhadi, "You only look once: Unified, real-time object detection," in *Proc. IEEE Conf. Comput. Vis. Pattern Recognit. (CVPR)*, Jun. 2016, pp. 779–788.

[31] Q. Mao, H. Sun, Y. Liu, and R. Jia, "Mini-YOLOv3: Real-time object detector for embedded applications," *IEEE Access*, vol. 7, pp. 133529–133538, 2019.

[32] M. Bjelonic. *YOLO ROS: Real-Time Object Detection for ROS*. Accessed: Jun. 30, 2021. [Online]. Available: https://github.com/leggedrobotics/darknet_ros

[33] V. Kazemi and J. Sullivan, "One millisecond face alignment with an ensemble of regression trees," in *Proc. IEEE Conf. Comput. Vis. Pattern Recognit.*, Jun. 2014, pp. 1867–1874.

[34] K. Khabarlak and L. Koriashkina, "Fast facial landmark detection and applications: A survey," *J. Comput. Sci. Technol.*, vol. 22, no. 1, pp. 12–41, 2022.
[35] S. G. Hart and L. E. Staveland, "Development of NASA-TLX (task load index): Results of empirical and theoretical research," in *Advances in Psychology*, vol. 52. Amsterdam, The Netherlands: Elsevier, 1988, pp. 139–183.
[36] J. Benesty, J. Chen, Y. Huang, and I. Cohen, "Pearson correlation coefficient," in *Noise Reduction in Speech Processing*. Berlin, Germany: Springer, 2009, pp. 1–4.

SOTIRIOS CHATZIDIMITRIADIS received the Diploma (M.Sc. equivalent) degree in electrical and computer engineering from the Aristotle University of Thessaloniki, Greece, in 2017. He is currently pursuing the Ph.D. degree with the University of Kent. He is also a Research Assistant with the Engineering Department, University of Kent, and a member of the Kent Assistive RObotics Laboratory (KAROL). His research interests include artificial intelligence, robotics, autonomous and assisted navigation systems, embedded systems, and computer vision.

SABER MIRZAEE BAFTI was born in Baft, Kerman, Iran, in 1989. He received the B.Sc. degree in electronic engineering from Chamran Technical and Vocational University, Iran, in 2010, and the M.Sc. degree in electronic engineering from the Sajad University of Technology, Iran, in 2014. He is currently pursuing the Ph.D. degree in electronic engineering with the University of Kent, U.K. He is also a member of the Kent Assistive Robotics Laboratory (KAROL). His research interests include computer vision, medical image processing, robotics, and embedded systems.

KONSTANTINOS SIRLANTZIS (Member, IEEE) is currently a Professor in applied artificial intelligence with the School of Engineering, Technology and Design, Canterbury Christ Church University (CCCU), Canterbury, Kent, U.K. He was an Associate Professor in intelligent systems with the School of Engineering, University of Kent, where he was the Head of the Robotics and Assistive Technologies Research Group and the Founding Director of the Kent Assistive RObotics Laboratory (KAROL). He has a strong track record in artificial intelligence and neural networks for image analysis and understanding, robotic systems with emphasis in assistive technologies, and pattern recognition for biometrics-based security applications. He has organized and chaired a range of international conferences and workshops, and he has authored over 150 peer-reviewed papers in journals and conferences.